



This is the author's version of a work that was accepted for publication in the following source:

Crea, K. N., Shivdasani, M. N., Argent, R. E., Mauger, S. J., Rathbone, G. D., O'Leary, S. J., & Paolini, A. G. (2009). Acute cochlear nucleus compression alters tuning properties of inferior colliculus neurons. *Audiology and Neurotology*, 15(1), 18-26.

Notice: Changes introduced as a result of publishing processes such as copy-editing and formatting may not be reflected in this document. For a definitive version of this work, please refer to the published source:

The final publication is available at *Audiology and Neurotology*:

<http://www.karger.com/Article/Abstract/218359>

Copyright of this article belongs to Karger Publishers, 2009

**Acute Cochlear Nucleus Compression Alters Tuning Properties of Inferior
Colliculus Neurons**

Katherine N. Crea^{1,2}, Mohit N. Shivdasani^{1,2,3}, Rebecca E. Argent², Stefan J. Mauger^{1,2,3},
Graeme D. Rathbone^{2,3}, Stephen J. O’Leary² & Antonio G. Paolini^{1,2}

¹School of Psychological Science, La Trobe University, Bundoora, VIC – 3086,
AUSTRALIA

²The Bionic Ear Institute, East Melbourne, VIC – 3002, AUSTRALIA

³Department of Electronic Engineering, La Trobe University, Bundoora, VIC – 3086,
AUSTRALIA

Running head: Midbrain Responses to Cochlear Nucleus Compression

Corresponding Author: Antonio G. Paolini,

School of Psychological Science

La Trobe University

Bundoora, VIC – 3086, AUSTRALIA.

Email: a.paolini@latrobe.edu.au

Tel: +61-3-94792947

Fax: +61-3-94791956

Abstract

Auditory Brainstem Implants (ABI) have been used in Neurofibromatosis type 2 (NF2) patients in an attempt to restore hearing sensation, with limited clinical success. Factors associated with poor clinical outcomes for NF2 ABI patients include larger tumour size, duration of hearing loss, and brainstem distortion and/or deformation caused by tumours that compress the brainstem. The present study investigated changes in tuning properties of inferior colliculus (IC) neurons following compression of the contralateral cochlear nucleus (CN). The left CN in adult rats ($n=8$) was exposed and a 32 channel acute recording probe inserted along the tonotopic gradient of the right IC. In four animals, an ethylene vinyl acetate (EVA) bead was applied to the exposed CN. Three recordings were made corresponding to $T_1=0$ min (before compression), $T_2=45$ min (during compression) and $T_3=225$ min (following bead removal/recovery). Recordings consisted of a response area protocol using pure tones of various frequencies and intensities (1-44 kHz; 10-70 dB SPL) to determine the characteristic frequency for each probe site. Compression of the CN led to sharpened tuning curves, decreased spike rate, and increased threshold and CF in the IC. Reversal of compression enabled these variables, excluding threshold, to recover to baseline. NF2 patients may have poorer ABI performance due to damage to the physical structure of the CN, resulting in alterations to the tonotopic organisation of the auditory pathway which may complicate ABI implantation and activation.

Keywords: Neurofibromatosis type 2, cochlear nucleus, inferior colliculus, compression, electrophysiology, tuning properties, auditory system.

INTRODUCTION

The Auditory Brainstem Implant (ABI) has been used to restore sound perception for patients who have had auditory nerve damage from the growth or removal of vestibular schwannomas (VS) caused by Neurofibromatosis type 2 (NF2) [Brackmann et al., 1993; Shannon et al., 1993]. Unfortunately speech perception following ABI implantation, without the use of lip reading, remains poor for these patients and is generally far below that observed for patients with cochlear implants [Otto et al., 2002; Schwartz et al., 2008]. One possible explanation for this poor performance is that VS damage the cochlear nucleus (CN) by compression and so subsequent electrical stimulation is of limited benefit [Matthies et al., 2000]. The present study investigates the impact of acute CN compression on auditory functioning in the inferior colliculus (IC) as a first step in modelling the potential physiological effects of compression caused by VS.

Clinical studies have investigated the association between various disease, electrode, and surgical factors and ABI outcomes for NF2 patients [e.g., Bouccara et al., 2007; Lesinski-Schiedat et al., 2000; Matthies et al., 2000]. More favourable ABI outcomes have been reported for NF2 patients with a shorter duration of hearing loss, smaller tumour size, and a higher number of active electrodes [Bouccara et al., 2007]. However, other studies have found no association between ABI outcomes and duration of hearing loss or tumour size [Lesinski-Schiedat et al., 2000]. Another potentially important factor in determining ABI outcomes for NF2 patients is brainstem compression. It has been reported that brainstem compression can lead to brainstem deformation and/or displacement, which can lead to

poorer overall ABI outcomes. Furthermore, it has been hypothesised that this may be caused by changes in the overall placement and distance between the cochlear nuclei, which may compromise the area available for stimulation. Clearly there are many complex and interacting factors that influence ABI outcomes for NF2 patients. Further investigations into the role of brainstem compression in ABI outcomes for NF2 patients may enhance our understanding [Matthies et al., 2000].

Although there are many complex factors that influence altered auditory functioning in NF2 patients, isolating acute CN compression influence is an important initial step in modelling the effects of this disease. The effect of CN compression on physiological functioning in the ascending auditory pathway has not been previously investigated. The present study investigated the electrophysiological and histological outcomes of acute CN compression. Specifically, this study investigated changes in tuning curve properties (characteristic frequency; threshold; sharpness of tuning and spike rate) that occurred in response to acute CN compression whilst controlling for the effect of changes over time. In addition, this study assessed whether release from compression reversed any observed changes, indicating recovery from compression. Finally, the effect of compression on the morphology of the CN was examined histologically.

MATERIALS AND METHODS

Surgery

Male Hooded Wistar rats (control/ no CN compression $n=4$; experimental $n=4$) of weight 250-500g were anaesthetised by intraperitoneal injection of Urethane in water (20% w/v; Sigma-Aldrich, NSW, Australia) at a dosage of 1.3-2.6 g/kg until an adequate depth of areflexia anaesthesia was achieved. Animals were placed in a stereotaxic frame and fitted with hollow ear bars (David Kopf Instruments, Tujunga, CA, USA). The left CN and contralateral IC were exposed by partial craniotomies and the dura mater patch over each site was then removed.

One 32-channel, acute recording probe (4 shanks each 5mm long and 200 μ m apart, each shank had 8 recording sites 200 μ m apart and with a surface area of 413 μ m²; NeuroNexus Technologies, Ann Arbor, MI, USA) was implanted into the exposed CNIC at a 10-15° rostral-caudal angle with a remote-controlled micromanipulator [Model MP-285, Sutter Instrument Company, CA, USA; as described in Shivdasani et al., 2008]. A low-impedance silver reference electrode was placed under the animal's skin at the back of the neck. The impedance of each electrode site at 1kHz was 1-3M Ω .

The cerebellum was aspirated to expose the left CN. For the experimental compression group, a non-biodegradable ethylene vinyl acetate (EVA) probe-mounted bead (weight 18 mg, length 4 mm, width 2 mm; DuPont™ Elvax® 40W, Melbourne, Australia) was applied to the lateral surface of the CN. Using a micro-manipulator the EVA bead was

slowly driven in a ventral direction until the CN was visually compressed under a microscope (8x magnification) and held in place by a manipulator arm mounted on the stereotaxic device (David Kopf Instruments, Tujunga, CA, USA).

The animal's temperature was maintained throughout the experimental and recording procedures at 37.5°C using a DC homoeothermic blanket (ATC1000, WPI, FL, USA). All surgical and electrophysiological recording procedures were conducted in a sound attenuating Faraday room, and carried out in accordance with the Australian NHMRC guidelines and AVRO standards and approved by the Animal Ethics Committee, St Vincent's Hospital, Melbourne, Australia (Protocol # 35/06 and 23/07).

Electrophysiological Recordings

A Tucker-Davis Technologies (TDT) System III hardware (TDT, FL, USA) was controlled with customised software written in OpenEx (TDT, FL, USA). This was employed to present acoustic stimuli throughout the experiment. An electrostatic speaker (Model EC1, TDT, FL, USA) was inserted into the left ear bar. Both the speaker and ear bar were calibrated before experiments commenced with a 1/8 inch condenser microphone (Brüel & Kjær, Nærum, Denmark). Tones at varying frequencies (1-44 kHz; 1 kHz steps) and intensities (10-70 dB sound pressure level (SPL); 10 dB SPL steps) were presented randomly through the left ear bar; each tone presented 20 times for 50 ms duration with a 5 ms rise/fall time and 300 ms inter-trial interval. In the experimental condition, the EVA bead was applied onto the CN following the initial recording ($T_1=0$ mins) at approximately 30-40 mins and removed following the second recording ($T_2=45$

mins) at approximately 210 mins. Post-compression recovery was assessed by a third and final recording ($T_3=225$ mins), with approximately 15 min of post-compression recovery time once the EVA bead was removed. At the conclusion of the experiment the EVA bead was reinserted for three animals in the experimental group prior to perfusion so that the state of the compressed CN could be analysed histologically. For one experimental animal the EVA bead was not replaced to investigate the shape of the CN upon recovery from compression.

Histological Analysis

Immediately following the final electrophysiological recording, rats were perfused transcardially with 4 % paraformaldehyde/PBS. The brains were stored at 4°C for 1-2 days in 0.4 % paraformaldehyde/PBS before being transferred to 30 % sucrose/PBS prior to cryostat sectioning (Model CM1850, Leica, Germany). Coronal 60 μ m serial sections were collected onto gelatin coated slides, stained for thionin and cover slipped with DPX histological mountant (Fluka, Switzerland). Sections were viewed and photographed in bright field using a Nikon Eclipse 90i D-PS Microscope and Nikon DS-SMC digital camera interfaced with NIS-elements software (Nikon, Japan).

Data Analysis

Acoustic Response Areas

Acoustic response areas for each frequency-intensity combination of sound presented in the first 0-50 ms from stimulus onset were constructed using TDT's OpenExplorer client-server application (TDT, FL, USA). Visual inspection of the acoustic response area was

made to determine characteristic frequency (CF) and threshold. Threshold was defined as the lowest intensity at which a unit responded and CF was defined as the frequency at which the unit responded at the lowest threshold. Total spike rate (spikes/sec) in the first 50 ms after stimulus onset was calculated at 30 dB SPL above threshold (Spikerate30), and at 70 dB SPL (Spikerate70), both at CF. Sharpness of tuning was defined as the quality factor, Q_n . Q_{10} , Q_{20} , and Q_{30} were used to quantify sharpness of tuning. They were calculated by dividing the CF by the bandwidth, 10, 20, or 30 dB SPL above threshold respectively. Broadly tuned units have Q_n values less than or equal to one, whereas sharply tuned units have Q_n values greater than one [Aitkin et al., 1975; Hernandez et al., 2005; Shivdasani et al., 2008].

Statistical Analyses

A mixed between-within-subjects design was utilised in this study to explore the differences between the control and experimental groups across three time points. Seven dependent variables were measured across each time point within group (producing a total of 21 variables): CF; threshold; Spikerate30; Spikerate70; and three measures of sharpness of tuning (Q_{10} , Q_{20} and Q_{30}).

Group within time effects were analysed for each variable utilising 2 x 2 (Group x Time) mixed between-within-subjects Analyses of Variance (ANOVAs) followed by simple main effects analyses of time within group where appropriate. Two ANOVAs were performed for each dependent variable as a result of substantial reduction in sample size and power due to missing data on some channels (e.g., for one animal in the control

group a recording at T₃ was not taken because the animal required euthanasia after T₂; some channels ceased to display driven multi-unit activity at T₂ and/or T₃, hence data could not be obtained; Spikerate30 could not be measured for those channels with thresholds greater than 50 dB SPL; all three Q_n values could only be measured for channels with thresholds less than or equal to 40 dB SPL). The effect of CN compression was assessed by analysing the differences between T₁ and T₂ between groups (referred to as the ‘compression’ condition) whereas recovery from compression was assessed by analysing the differences between T₁ and T₃ between groups (referred to as the ‘recovery’ condition). Since this statistical procedure analyses the differences between the various time points for each channel, only channels that included data for T₁ and T₂ (compression condition) and T₁ and T₃ (recovery condition) would have been included in the ANOVAs. Taking this into account, means and standard errors included in Figure 4 are displayed for only channels that included data for all three time points for each variable (44 control channels, 35 experimental channels). This subsample is more representative of the data that would have been included in each ANOVA than the overall means and standard errors for all channels. It is important to note that the *difference* between the means is what is of interest, rather than the mean itself since this study utilised a repeated measures design. Since the subsample of complete data is smaller, the standard errors are larger.

A Bonferroni correction was applied, reducing the critical p value for statistical significance to .0036 for all analyses, maintaining the overall type I error rate at .05. Data was entered into SPSS (Version 14.0; SPSS Inc., IL, USA) for analysis.

RESULTS

A maximum of 32 channels of data were obtained from each animal (maximum total of 128 control and 128 experimental channels). Channels that did not show driven multi-unit activity ($n = 65$) were excluded from the final data set because no measure of CF could be obtained (only spontaneous activity was present on these channels). Inspection of box-plots of each variable within group revealed three outliers that were removed before ANOVAs were conducted. The final data set comprised 101 experimental channels and 87 control channels of which 15 channels produced multi-peaked tuning curves (3 experimental, 12 control). For these channels, the CF was measured for the peak with the lowest threshold [Hernandez et al., 2005].

Histology

Electrode placements were identified within the CNIC in each implanted animal. Figure 1A is a schematic diagram showing the position of identified electrode placements for all experiments (open symbols represent the control group and filled symbols represent the experimental group), demonstrating that the majority of electrode placements are within the borders of the CNIC. An example of the IC (coronal section) from an experimental animal in which the position of the four electrode placements have been identified and are marked with arrows is shown in Figure 1B. Outlines of the IC and its subdivisions were determined upon reference to the rat brain atlas [Paxinos and Watson, 2005].

The morphology of the compressed experimental CN was compared qualitatively with that of the non-operated control side for each animal. The CN in which the EVA bead remained in place during perfusion, shows the extent of the compression effect. The CN has been compressed in the lateral-medial and dorsal-ventral direction (compare Figure 2A with 2B). The position of the EVA bead *in vivo* can be seen in Figure 2A (in an animal where the bead was removed post-mortem). Removal of the EVA bead *in vivo* allowed the compressed CN to return to its former dimensions (Figure 2C). The CN has returned to the ‘normal’ control morphology seen in the non-compressed/non-operated CN shown in Figure 2D. The outline of the CN was determined upon reference to the rat brain atlas [Paxinos and Watson, 2005].

Characteristic Frequency

The control group’s CF was found to remain stable over time (Figure 4A, upper panel; Figure 3A) while the application of CN compression in the experimental group resulted in an overall shift in CF towards higher frequencies (Figure 4A, lower panel; Figure 3B). The mean increase in CF for the experimental group was 2.66 kHz (Standard Error (SE) = 0.42 kHz). Such changes were reflected in a significant main effect of time in the compression condition ($n = 87$ control, $n = 85$ experimental), $F(1, 170) = 20.58$, $p < .001$, partial $\eta^2 = 0.11$, $1 - \beta = 1.00$, and a significant time by group interaction effect, $F(1, 170) = 29.46$, $p < .001$, partial $\eta^2 = 0.15$, $1 - \beta = 1.00$. Simple main effects analyses of time within group revealed a significant difference between T₁ and T₂ for the experimental group only (Figure 4A, lower panel), $F(1, 170) = 49.07$, $p < .001$, partial $\eta^2 = 0.22$, $1 - \beta = 1.00$. Main effects were not observed in the recovery condition ($n = 61$

control, $n = 66$ experimental), indicating that both groups had returned to baseline CF levels at T_3 (Figure 4A, compare T_1 with T_3 for control and experimental groups).

Threshold

The control group showed relatively stable threshold levels over time, with a slight increase in threshold at T_3 (Figure 4B, upper panel), whereas the experimental group showed an overall increase in threshold due to CN compression, which was still statistically significant from T_1 at T_3 (Figure 4B, lower panel). The mean increase in threshold due to CN compression for the experimental group was 5.71 dB SPL ($SE = 1.49$ dB SPL). These changes were reflected in a significant main effect of time in the compression condition ($n = 87$ control, $n = 87$ experimental), $F(1, 172) = 69.43$, $p < .001$, partial $\eta^2 = 0.29$, $1 - \beta = 1.00$, and a significant time by group interaction effect, $F(1, 172) = 63.46$, $p < .001$, partial $\eta^2 = 0.27$, $1 - \beta = 1.00$. Simple main effects analyses of time within group revealed a significant difference between T_1 and T_2 for the experimental group only (Figure 4B, lower panel), $F(1, 172) = 132.82$, $p < .001$, partial $\eta^2 = 0.44$, $1 - \beta = 1.00$. In the recovery condition ($n = 61$ control, $n = 66$ experimental), a main effect of time was observed, $F(1, 125) = 35.60$, $p < .001$, partial $\eta^2 = 0.22$, $1 - \beta = 1.00$ but an interaction effect was not observed, indicating that the control and experimental groups showed a similar pattern of change in threshold. Simple main effects analyses of time within group showed that the control and experimental groups had increased mean threshold from baseline, $F(1, 125) = 10.40$, $p = .002$, partial $\eta^2 = 0.08$, $1 - \beta = 0.89$; $F(1, 125) = 27.62$, $p < .001$, partial $\eta^2 = 0.18$, $1 - \beta = 1.00$, respectively (Figure 4B, compare T_1 with T_3).

Spike rate

The control group showed relatively stable spike rates over time (Figure 4C, upper panel; Figure 3A) whereas the experimental group showed a large decrease in spike rate at T₂ followed by an increase in spike rate to approximately baseline levels at T₃ (Figure 4C, lower panel; Figure 3B). Mean decrease in spike rate in the compression condition was 46.31 spikes/sec ($SE = 12.87$ spikes/sec), and 54.06 spikes/sec ($SE = 14.74$ spikes/sec), for Spikerate30 and Spikerate70, respectively. These results were reflected in a significant main effect of time in the compression condition for Spikerate30 ($n = 57$ control, $n = 65$ experimental), $F(1, 120) = 30.50$, $p < .001$, partial $\eta^2 = 0.20$, $1 - \beta = 1.00$; and Spikerate70 ($n = 86$ control, $n = 99$ experimental), $F(1, 183) = 57.06$, $p < .001$, partial $\eta^2 = 0.24$, $1 - \beta = 1.00$. Significant time by group interaction effects were also observed, indicating a different pattern of change over time for the control and experimental groups, for Spikerate30, $F(1, 120) = 50.79$, $p < .001$, partial $\eta^2 = 0.30$, $1 - \beta = 1.00$; and Spikerate70, $F(1, 183) = 91.24$, $p < .001$, partial $\eta^2 = 0.33$, $1 - \beta = 1.00$. Simple main effects analyses of time within group showed a significant difference between T₁ and T₂ for the experimental group only for both Spikerate30, $F(1, 120) = 85.62$, $p < .001$, partial $\eta^2 = 0.42$, $1 - \beta = 1.00$; and Spikerate70, $F(1, 183) = 157.36$, $p < .001$, partial $\eta^2 = 0.46$, $1 - \beta = 1.00$ (Figure 4C, compare T₁ with T₂, lower panel). Main effects were not observed in the recovery condition for Spikerate30 ($n = 48$ control, $n = 53$ experimental) and Spikerate70 ($n = 63$ control, $n = 69$ experimental), indicating that all groups had returned to baseline spike rate levels at T₃ (Figure 4C, compare T₁ with T₃ for control and experimental groups).

Sharpness of Tuning

Results from the control group indicated that sharpness of tuning remained relatively stable over time (Figure 4D, upper panel; Figure 3A). For the three measures of sharpness of tuning, Q_{10} , Q_{20} , and Q_{30} , the experimental group was more sharply tuned at T_2 compared with baseline (Figure 4D, lower panel; Figure 3B). Sharpness of tuning returned to approximately baseline levels once compression was removed, indicating that recovery from compression had occurred (Figure 4D). In order, mean increase in Q values in the compression condition for Q_{10} , Q_{20} , and Q_{30} , were 1.23 ($SE = 0.29$); 0.62 ($SE = 0.17$); and 0.53 ($SE = 0.11$). These results were reflected in a significant main effect for time in the compression condition for Q_{10} ($n = 85$ control, $n = 82$ experimental), $F(1, 165) = 32.13$, $p < .001$, partial $\eta^2 = 0.16$, $1 - \beta = 1.00$; Q_{20} ($n = 72$ control, $n = 73$ experimental), $F(1, 143) = 34.25$, $p < .001$, partial $\eta^2 = 0.19$, $1 - \beta = 1.00$; and Q_{30} ($n = 57$ control, $n = 54$ experimental), $F(1, 109) = 39.77$, $p < .001$, partial $\eta^2 = 0.27$, $1 - \beta = 1.00$. Time by group interaction effects were also observed, indicating that there was a different pattern of change for the control and experimental groups over these two time points for Q_{10} , $F(1, 165) = 34.44$, $p < .001$, partial $\eta^2 = 0.17$, $1 - \beta = 1.00$; Q_{20} , $F(1, 143) = 39.69$, $p < .001$, partial $\eta^2 = 0.22$, $1 - \beta = 1.00$; and Q_{30} , $F(1, 109) = 53.05$, $p < .001$, partial $\eta^2 = 0.33$, $1 - \beta = 1.00$. Simple main effects analyses of time within group showed a significant difference between T_1 and T_2 for the experimental group only for Q_{10} , $F(1, 165) = 65.37$, $p < .001$, partial $\eta^2 = 0.28$, $1 - \beta = 1.00$; Q_{20} , $F(1, 143) = 74.35$, $p < .001$, partial $\eta^2 = 0.34$, $1 - \beta = 1.00$; and Q_{30} , $F(1, 109) = 89.92$, $p < .001$, partial $\eta^2 = 0.45$, $1 - \beta = 1.00$ (Figure 4D, compare T_1 with T_2 , lower panel). Main effects were not observed for the recovery

condition for Q_{10} ($n = 61$ control, $n = 65$ experimental), Q_{20} ($n = 54$ control, $n = 61$ experimental), and Q_{30} ($n = 45$ control, $n = 50$ experimental), indicating that the control and experimental groups had returned to baseline sharpness of tuning levels at T_3 (Figure 4D, compare T_1 with T_3 for control and experimental groups).

DISCUSSION

The objective of this study was to investigate the impact of acute CN compression on auditory electrophysiological functioning in the IC. The corresponding changes in the gross anatomy of the CN were also investigated. Our findings indicate that compression of the CN altered tuning properties of IC neurons: sharpened tuning curves, decreased spike rate, increased threshold, and increased CF. In addition, during compression, the CN became elongated and compacted compared to the non-operated contralateral control side. Release from compression resulted in the return of IC tuning properties, except threshold, to baseline values which were reflected in the recovery of CN morphology.

One possible explanation for the observed changes reported in the present study is that compression of the CN may lead to reduction of its afferent blood supply which could reduce the overall excitatory drive from the CN to ascending auditory pathways through a shift in the balance of energy substrates. The balance between inhibition and excitation plays a pivotal role in shaping the response properties of auditory neurons [Paolini et al., 2004, 2005; Nayagam et al., 2005, 2006], and blocking inhibition has been shown to increase spike rate, decrease threshold, and increase the excitatory response area in the primary auditory cortex [Wang et al., 2000]. The observed changes in IC tuning properties – sharpened tuning curves, decreased spike rate, increased threshold, and increased CF – are consistent with this proposed hypothesis, an increase in inhibitory neurotransmission following a reduction in blood supply to the CN. Although markers of an ischemic insult were not directly measured in the present study, it is plausible that

compression of the CN may have impeded blood flow to this structure resulting in the observed changes in the IC. Indeed NF2 VS can share their blood supply with the CN and it has been hypothesised that this may alter local vascularisation [Colletti and Shannon, 2005]. An important control condition for future studies would be to directly restrict blood flow to the CN and observe whether IC tuning properties change in a similar fashion to those observed following acute CN compression.

Recovery of IC tuning properties to baseline values was observed for all variables, excluding threshold. Although thresholds approached baseline levels after compression was removed, a significant difference was still observed between baseline and recovery, however, this effect was also observed for the control group. The observed recovery effect may be explained by the restoration of blood supply to the CN and ensuing excitatory drive to the IC after release from compression.

Some NF2 patients experience progressive sensorineural hearing loss with disease progression, whereas others have normal hearing, even with tumours larger than 4cm [Colletti and Shannon, 2005; Kanowitz et al., 2004]. Once implanted with an ABI, there is large variability in outcomes. Interestingly, tumour size does not always relate to ABI outcomes [Lesinski-Schiedat et al., 2000]. Rather, the resulting impact of brainstem compression on the cochlear nuclei may account for the varying ABI outcomes for NF2 patients with different tumour sizes. If the brainstem can be successfully decompressed after resection of VS and the cochlear nuclei are relatively intact, pre-existing brainstem compression may not cause poor ABI outcomes. If brainstem compression causes

distortion of the brainstem, the cochlear nuclei may be more difficult to stimulate successfully with an ABI and hence lead to poorer outcomes. The relationship between compression effects and ABI outcomes for NF2 patients warrants further clinical investigation [Matthies et al., 2000].

The findings of the present study suggest that CN compression may play a role in auditory dysfunction observed in NF2 patients. The observed changes in tuning properties in the IC would affect hearing by decreasing sensitivity to lower frequencies and generally decreasing sensitivity to auditory stimuli due to increased thresholds and decreased spike rate. The increased sharpness in tuning may affect the processing of more complex sounds such as speech. The observed changes in tuning properties of IC neurons may be reflected long-term in an overall change in the way sound is mapped in the auditory system. Once implanted with an ABI, stimulation parameters would need to be tailored to this altered tonotopic map.

One must be mindful of the important differences between the present model of CN compression and the development of VS in NF2 patients, including the time course over which the CN becomes compressed, and the fact that the EVA bead is hard whereas tumours are soft-tissue. In the present study we acutely compressed the CN, whereas VS grow over time and may take months or years to become large enough to compress the CN [Mirz et al., 2000]. This study has shown that acute CN compression is enough to cause changes in the tuning of IC neurons which suggests a role for compression in the development of altered auditory sensation in NF2 patients. A model of chronic CN

compression would be an important advancement in our understanding of NF2 to assess the plastic changes elicited in the ascending auditory pathways and to explore whether these changes are less susceptible to reversal once compression is released. Alterations to the tonotopic map in the IC could be assessed in a chronic model of CN compression to provide insight into possible mechanisms of progressive hearing loss with VS growth.

The results presented here suggest a role for CN compression in the development of hearing loss with VS in NF2 patients. We conclude that acute CN compression leads to substantial, yet reversible changes in tuning properties in the IC. This may have implications for the implantation and activation of ABI electrodes and stimulation parameters, affecting the overall hearing outcomes for NF2 patients.

REFERENCES

Aitkin LM, Webster WR, Veale JL, Crosby DC: Inferior colliculus. I. Comparison of response properties of neurons in central, pericentral, and external nuclei of adult cat. *J Neurophysiol* 1975; 38: 1196-1207.

Bouccara D, Kalamarides M, Bozorg Grayeli A, Ambert-Dahan E, Rey A, Sterkers O: Implant auditif du tronc cerebral: Indications et resultats. *Annales d'Otolaryngologie et chirurgie cervico-faciale*; 124: 148-154.

Brackmann DE, Hitselberger WE, Nelson RA, Moore J, Waring MD, Portillo F, Shannon RV, Telischi FF: Auditory brainstem implant: I. Issues in surgical implantation. *Otolaryngol Head Neck Surg* 1993; 108:624-633.

Colletti V, Shannon, RV: Open set speech perception with auditory brainstem implant? *Laryngoscope* 2005; 115: 1974-1978.

Hernandez O, Espinosa N, Perez-Gonzalez D, Malmierca MS: The inferior colliculus of the rat: A quantitative analysis of monaural frequency response areas. *Neuroscience* 2005; 132: 203-217.

Kuchta J: Twenty-five years of auditory brainstem implants: perspectives. *Acta Neurochir Suppl* 2007; 97: 443-449.

Lesinski-Schiedat A, Frohne C, Illg A, Rost U, Matthies C., Battmer RD, Samii M, Lenarz T: Auditory brainstem implant in auditory rehabilitation of patients with neurofibromatosis type 2: Hannover programme. *J Laryngol Otol*; 114: 15-17.

Matthies C, Thomas S, Moshrefi M, Lesinski-Schiedat A, Frohne C, Battmer RD, Lenarz T, Samii M: Auditory brainstem implants: current neurosurgical experiences and perspective. *J Laryngol Otol* 2000; 114: 32-36.

Mirz F, Pedersen CB, Fiirgaard B, Lundorf E: Incidence and growth pattern of vestibular schwannomas in a Danish County, 1977-98. *Acta Otolaryngol* 2000; 543: 30-33.

Nayagam DA, Clarey JC, Paolini AG: Powerful, onset inhibition in the ventral nucleus of the lateral lemniscus. *J Neurophysiol* 2005; 94:1651-1654.

Nayagam DA, Clarey JC, Paolini AG. Intracellular responses and morphology of rat ventral complex of the lateral lemniscus neurons in vivo. *J Comp Neurol* 2006; 498:295-315.

Otto SR, Brackmann DE, Hitselberger WE, Shannon RV, Kutchta J: Multichannel auditory brainstem implant: update on performance in 61 patients. *J Neurosurg* 2002; 96: 1063-1071.

Paolini AG, Clarey JC, Needham K, Clark GM: Fast inhibition alters first spike timing in auditory brainstem neurons. *J Neurophysiol* 2004; 92:2615-2621.

Paolini AG, Clarey JC, Needham K, Clark GM: Balanced inhibition and excitation underlies spike firing regularity in ventral cochlear nucleus chopper neurons. *Eur J Neurosci* 2005; 21:1236-1248.

Paxinos G, Watson C: *The rat brain in stereotaxic coordinates*. 5th ed., San Diego, Academic Press, 2005.

Schwartz MS, Otto SR, Shannon RV, Hitselberger WE, Brackmann DE: Auditory brainstem implants. *Neurotherapeutics* 2008; 5: 128-136.

Shannon RV, Fayad J, Moore J, Lo WW, Otto S, Nelson RA, O'Leary M: Auditory brainstem implant: II. Postsurgical issues and performance. *Otolaryngol Head Neck Surg* 1993; 108: 634-642.

Shivdasani MN, Mauger SJ, Rathbone GD, Paolini AG: Inferior colliculus responses to multichannel microstimulation of the ventral cochlear nucleus: Implications for Auditory Brainstem Implants. *J Neurophysiol* 2008; 99: 1-13.

Wang J, Caspary D, Salvi RJ: GABA-A antagonist causes dramatic expansion of tuning in primary auditory cortex. *Neuroreport* 2000; 11: 1137-1140.

Acknowledgments

We thank Courtney Suhr for her technical assistance. We would also like to acknowledge Dr. Ben Ong and Dr. Melanie Murphy for their advice regarding data analysis. This project was supported by the Garnett Passe and Rodney Williams Memorial Foundation. Research was conducted at the Auditory Clinical Neuroscience Unit, The Bionic Ear Institute, Melbourne, Australia.

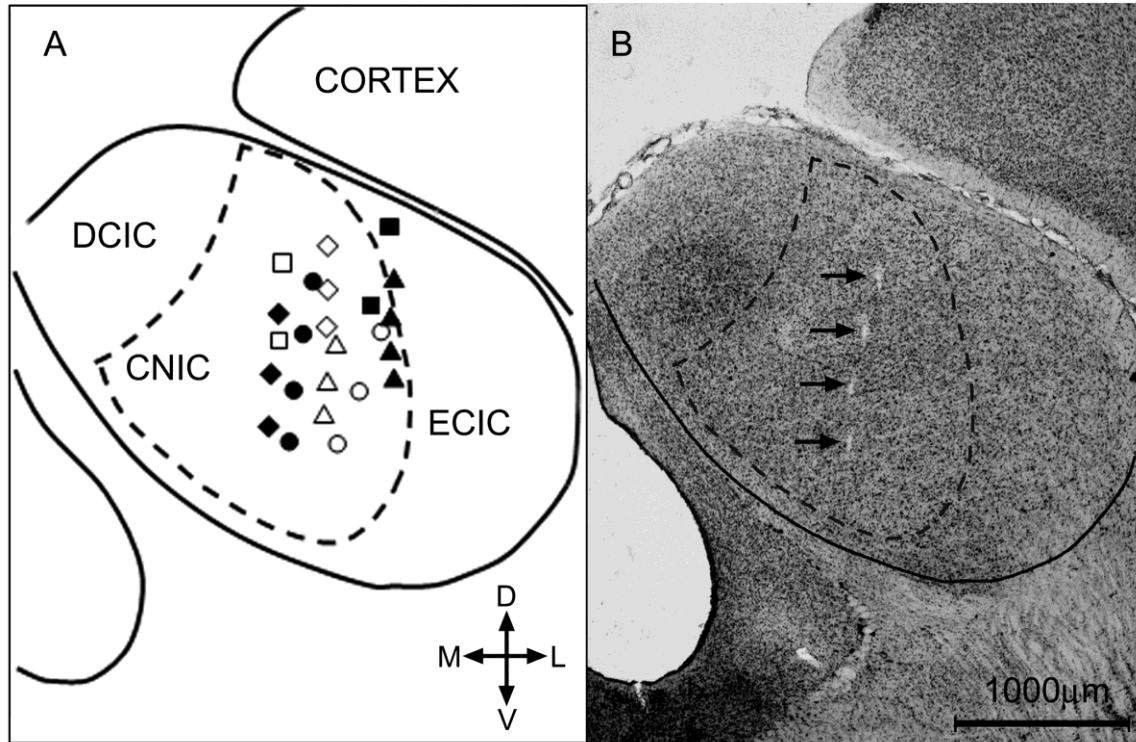


Figure 1

Figure 1. Verification of electrode probe placement in the IC. Broken lines indicate the subdivisions of the IC (central nucleus (CNIC), dorsal cortex (DCIC), and external cortex of the IC (ECIC). Solid lines demarcate the border of the IC. A: Schematic diagram of IC electrode placements identified in each animal compiled from histological sections. Each electrode probe placement is represented by a unique symbol; filled symbols represent the animal from the experimental group, open symbols represent the control animals. Note that the majority of the electrode placements were within the CNIC. B: Bright field image of the IC from an experimental animal in the coronal plane stained with thionin, (2 x magnification). Arrows denote the positions of the four shanks of the electrode probe.

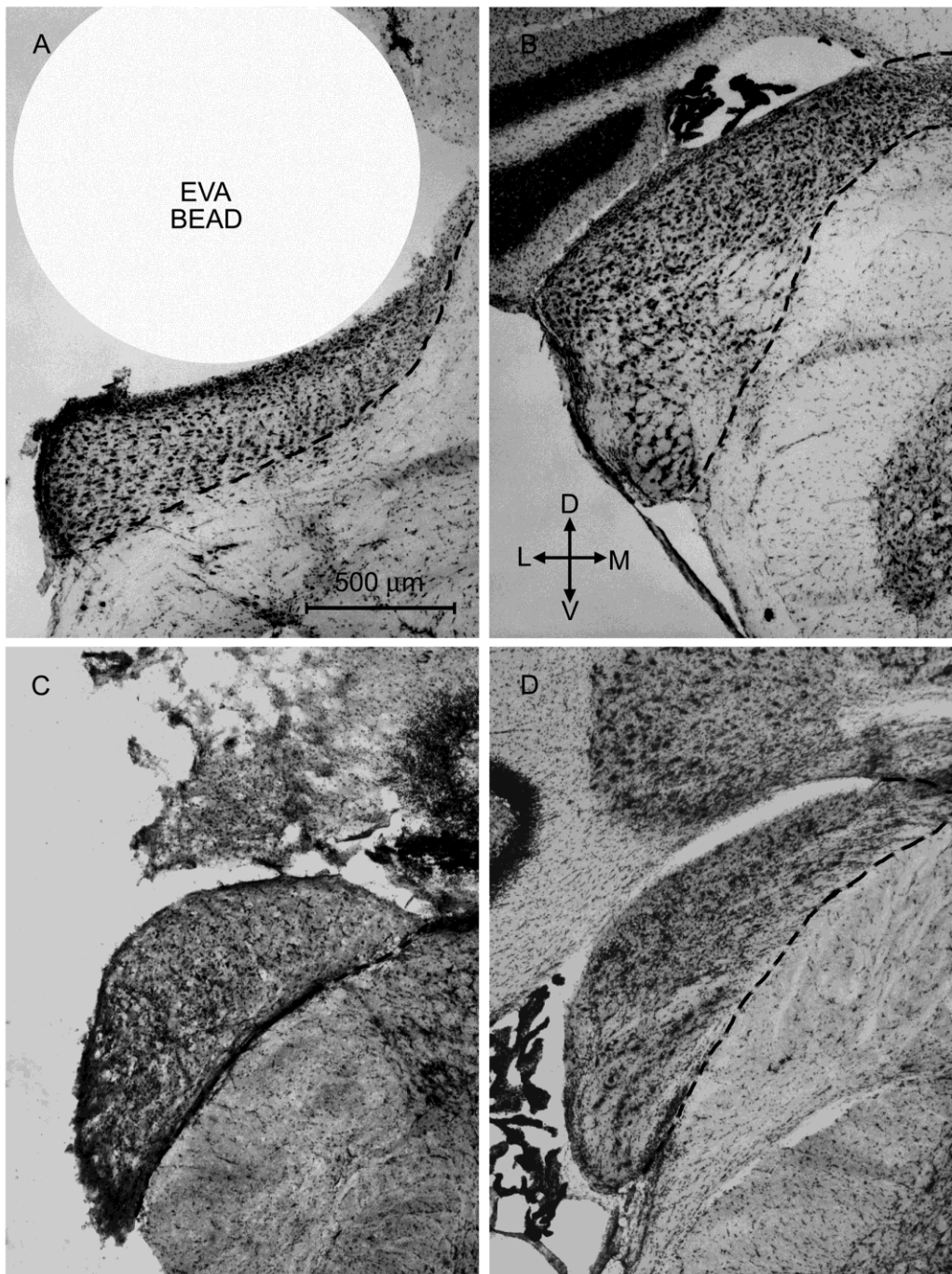


Figure 2

Figure 2. Examples of thionin stained sections (in the coronal plane) showing paired cochlear nuclei (CN), of equivalent coronal level, from two experimental animals (4x

magnification). Broken lines indicate the border of the CN. A-B: CN pairs from one experimental animal perfused with the EVA bead *in situ*. A: shows the morphology of the compressed left CN and the approximate position of the EVA bead (EVA bead not to scale; see main text). B: shows the non-operated (right) control CN. C-D: CN pairs from a second experimental animal in which the EVA bead was removed prior to perfusion. C: shows the experimental (left) CN following the removal of the EVA bead illustrating the extent of post-compression recovery observed. D: shows the non-operated (right) control CN.

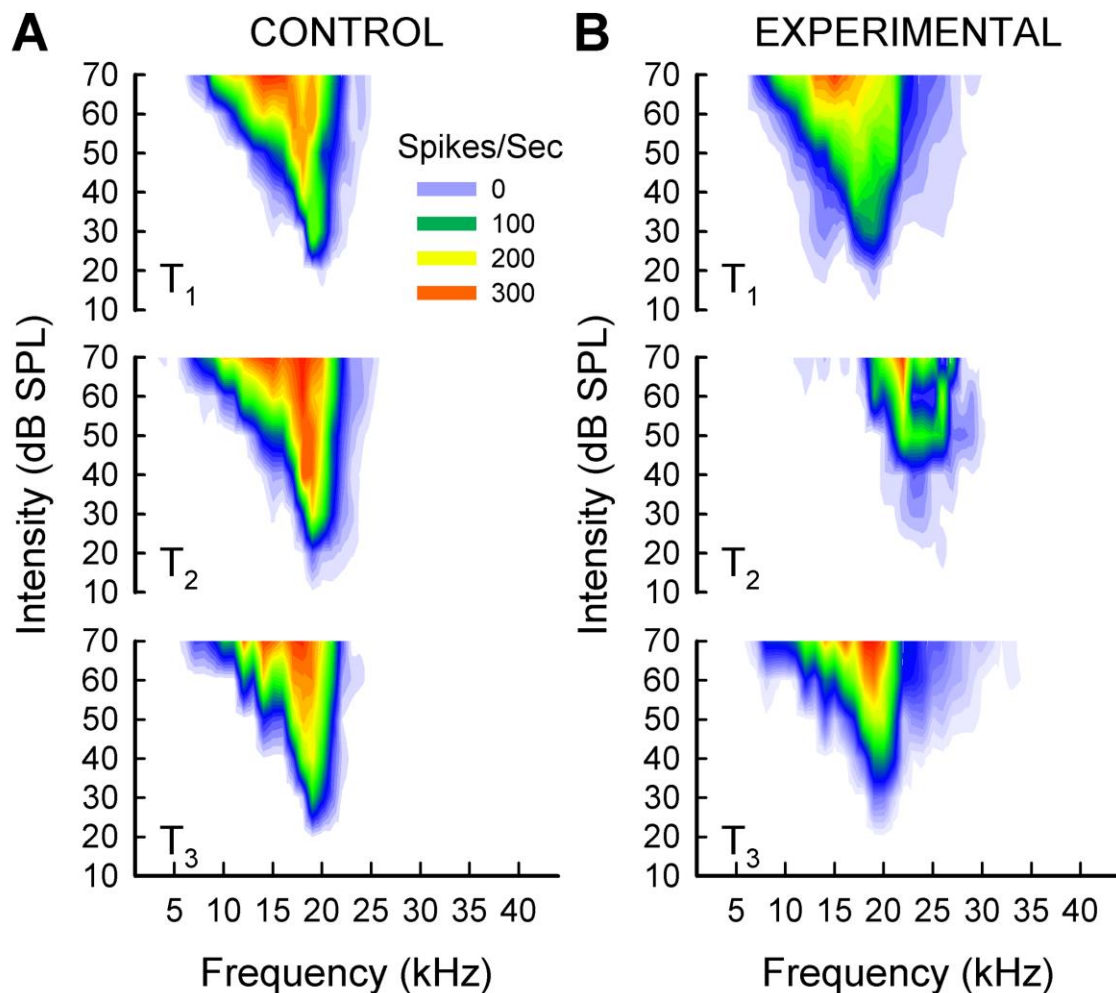


Figure 3

Figure 3. A: Acoustic response area examples from one recording channel for a control animal, showing no change in tuning from T_1 to T_3 . B: Acoustic response area examples from one recording channel for an experimental animal, showing an increase in CF and threshold, a decrease in spike rate, and a sharpening of tuning from T_1 to T_2 , followed by a return in tuning properties to approximately baseline levels at T_3 . A-B: Colours represent spike rate (spikes/sec); maximum spike rate is coloured red whereas lowest spike rate is coloured pale blue (key).

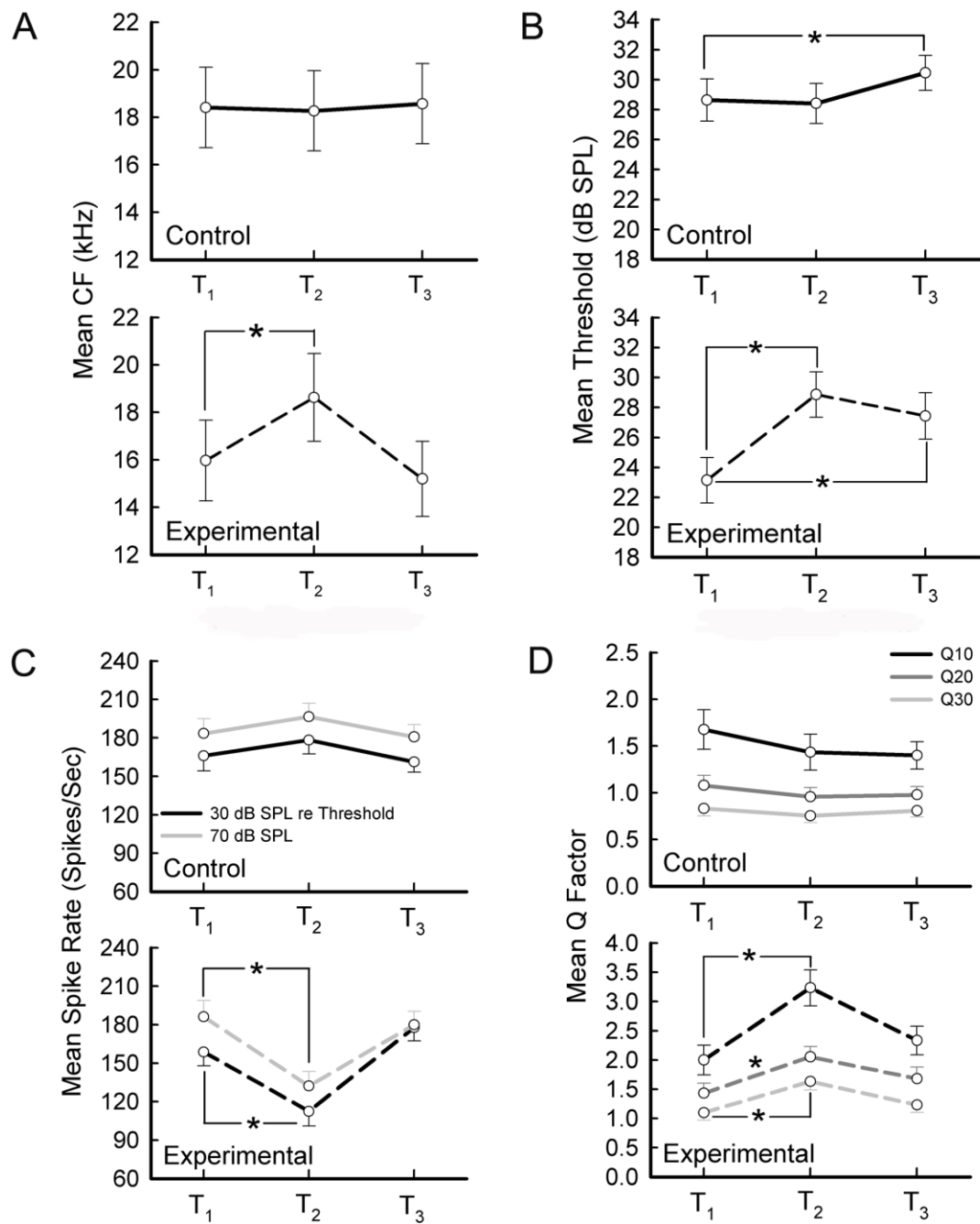


Figure 4

Figure 4. A: Means and SEs for CF over three recording times (T₁, T₂, T₃) for both control (solid lines) and experimental (dashed lines) groups. Note that in the experimental group a significant difference (*) was found in mean CF between T₁ and T₂ ($p < .001$).

B: Means and SEs for threshold over three recording times (T_1 , T_2 , T_3) for both control (solid lines) and experimental (dashed lines) groups. Note that in the experimental group a significant difference (*) was found in mean threshold between T_1 and T_2 . Both the control and experimental groups showed a significant difference (*) in mean threshold between T_1 and T_3 ($p=.002$, $p<.001$ respectively).

C: Means and SEs for spike rate over three recording times (T_1 , T_2 , T_3) for both control (solid lines: black line represents spike rate 30 dB SPL above threshold; grey line represents spike rate at 70 dB SPL) and experimental (dashed lines: black dashed line represents spike rate 30 dB SPL above threshold; grey dashed line represents spike rate at 70 dB SPL) groups. Note that in the experimental groups a significant difference (*) was found in mean spike rate between T_1 and T_2 ($p<.001$).

D: Means and SEs for sharpness of tuning over three recording times (T_1 , T_2 , T_3) for both control (solid lines: black line represents Q_{10} ; medium grey line represents Q_{20} ; pale grey line represents Q_{30}) and experimental (dashed lines: black dashed line represents Q_{10} ; medium grey dashed line represents Q_{20} ; pale grey line represents Q_{30}) groups. Note that in the experimental groups a significant difference (*) was found in mean sharpness of tuning between T_1 and T_2 ($p<.001$).